J|A|C|S ARTICLES

Published on Web 06/04/2009

The Tetracyanopyrazinide Dimer Dianion, $[TCNP]_2^{2-}$. 2-Electron 8-Center Bonding

Juan J. Novoa,*,† Peter W. Stephens,*,‡ Mahika Weerasekare,§ William W. Shum,§ and Joel S. Miller*,§

Department of Physics & Astronomy, Stony Brook University, Stony Brook, New York 11794-3800, Departament de Química Física and IQTCUB, Facultat de Química, Universitat de Barcelona, Av. Diagonal 647, 08028-Barcelona, Spain, and Department of Chemistry, 315 S. 1400 E. RM 2124, University of Utah, Salt Lake City, Utah 84112-0850

Received April 7, 2009; E-mail: juan.novoa@ub.edu; Peter.Stephens@sunysb.edu; jsmiller@chem.utah.edu

Abstract: The reaction of $Cr(C_6H_6)_2$ and 1,2,4,5-tetracyanopyrazine (TCNP) forms $[Cr(C_6H_6)_2][TCNP]$, and TCNP is reduced and forms the eclipsed π-$[TCNP]_2^{2-}$ dimer. Diamagnetic $[TCNP]_2^{2-}$ has an intradimer separation of 3.14(2) Å. The intradimer C···C and N···N separations are 3.29(2) and 3.42(2) Å, respectively, and increase with the distance from the center of the molecule, due to nitriles bending away from the plane of the molecule by $5 \pm 1°$. $[TCNP]_2^{2-}$ is best described by an atoms-in-molecules analysis as having a $2e^-$/8c C−C bond involving the four C atoms from each six-member ring. The results of B3LYP/6-31+G(d)-computed interactions indicate that the $[TCNP]^{\bullet-}$···$[TCNP]^{\bullet-}$ interactions in an isolated $[TCNP]_2^{2-}$ are repulsive by 58.9 kcal/mol, and that the stability of $[TCNP]_2^{2-}$ primarily originates from $[TCNP]^{\bullet-}$···$cation^+$ electrostatic interactions, whose sum (−209.8 kcal/mol) exceeds the sum of the repulsive $[TCNP]^{\bullet-}$···$[TCNP]^{\bullet-}$ and $cation^+$···$cation^+$ interactions (140.3 kcal/mol).

Introduction

Electron poor cyanocarbons form numerous Mulliken donor−acceptor complexes,[1] and frequently form radical anions that are stabilized via charge and spin delocalization. This is the basis for numerous stable electron transfer salts that have been characterized to exhibit technologically important properties such as magnetic ordering,[2] metal-like electrical conductivity[3] and even superconductivity.[4] In the former case, for example, the reaction of $V(CO)_6$ with TCNE (tetracyanoethylene),[5,6] TCNQ (7,7,8,8-tetracyano-*p*-quinodimethane),[7] TCNB (1,2,4,5-tetracyanobenzene),[8a] and TCNP (1,2,4,5-tetracyanopyrazine),[9] forms organic-based magnets with magnetic ordering temperatures exceeding room temperature.

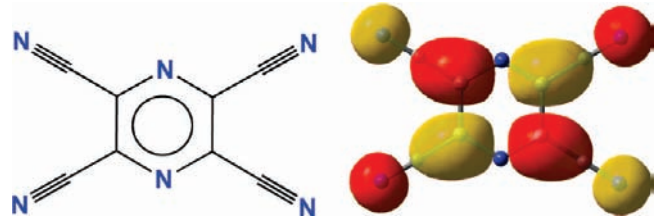

Some of these electron transfer salts, however, do not exhibit collective electronic properties, as they form closed-shell singlet (diamagnetic) dimeric dianions with exceptionally long, in-

† Universitat de Barcelona.
‡ Stony Brook University.
§ University of Utah.

(1) E.g.: (a) Mulliken, R. S.; Person, W. B. *Molecular Complexes: A Lecture and Reprint Volume*; Wiley: New York, 1969.
(2) E.g.: (a) Ovcharenko, V. I.; Sagdeev, R. Z. *Russ. Chem. Rev.* **1999**, *68*, 345. Kinoshita, M. *Philos. Trans. R. Soc. London, A* **1999**, *357*, 2855. (b) Miller, J. S.; Epstein, A. J. *Angew. Chem., Int. Ed.* **1999**, *33*, 385. Miller, J. S.; Epstein, A. J. *Chem. Eng. News* **1995**, *73* (40), 30. (c) Blundell, S J.; Pratt, F, P. *J. Phys.: Condens. Matter* **2004**, *16*, R771. Crayson, J. A.; Devine, J. N.; Walton, J. C. *Tetrahedron* **2000**, *56*, 7829.
(3) E.g.: Skotheim, T. A.; Elsenbaumer, R. L.; Reynolds, J. R., Eds. *Handbook of conducting polymers*, 2nd ed.; M. Dekker: New York, 1998. Ferraro, J. R.; Williams, J. M. *Introduction to synthetic electrical conductors*; Academic Press: Orlando, 1987.
(4) E.g.: Williams, J. M. *Organic superconductors (including fullerenes): synthesis, structure, properties, and theory*; Prentice Hall: Englewood Cliffs, NJ, 1992. Ishiguro, T.; Yamaji, K.; Saito, S. *Organic superconductors*; Springer: New York, 1998.
(5) Miller, J. S. *Angew. Chem., Int. Ed.* **2006**, *45*, 2508; *Angew. Chem.* **2006**, *117*, 2570.
(6) (a) Manriquez, J. M.; Yee, G. T.; McLean, R. S.; Epstein, A. J.; Miller, J. S. *Science* **1991**, *252*, 1415. Miller, J. S.; Yee, G. T.; Manriquez, J. M.; Epstein, A. J. In *Proceedings of Nobel Symposium #NS-81 Conjugated Polymers and Related Materials: The Interconnection of Chemical and Electronic Structure*; Salaneck, W. R., Lundström, I., Råbny, B., Eds.; Oxford Univ. Press: Oxford, 1993; p 461. (b) Zhang, J.; Zhou, P.; Brinckerhoff, W. B.; Epstein, A. J.; Vazquez, C.; McLean, R. S.; Miller, J. S. *ACS Symp. Ser.* **1996**, *644*, 311.
(7) Vickers, E. B.; Selby, T. D.; Thorum, M. D.; Taliaferro, M. L.; Miller, J. S. *Inorg. Chem.* **2004**, *43*, 6414.
(8) (a) Taliaferro, M. L.; Thorum, M. S.; Miller, J. S. *Angew. Chem., Int. Ed.* **2006**, *45*, 5326. (b) Bagnato, J. D.; Shum, W. W.; Strohmeier, M.; Grant, D. M.; Arif, A. M.; Miller, J. S. *Angew. Chem., Int. Ed.* **2006**, *45*, 5322.
(9) Vickers, E. B.; Selby, T. D.; Miller, J. S. *J. Am. Chem. Soc.* **2004**, *126*, 3716.
(10) (a) Del Sesto, R. E.; Miller, J. S.; Novoa, J. J.; Lafuente, P. *Chem.—Eur. J.* **2002**, *8*, 4894. (b) Miller, J. S.; Novoa, J. J. *Acc. Chem. Res.* **2007**, *40*, 189. (c) Garcia-Yoldi, I.; Miller, J. S.; Novoa, J. J. *Phys. Chem. Chem. Phys.* **2008**, *10*, 4106. (d) Garcia-Yoldi, I.; Miller, J. S.; Novoa, J. J. *J. Phys. Chem. A* **2009**, *113*, 484. (e) Goto, K.; Kubo, T.; Yamamoto, K.; Nakasuji, K.; Sato, K.; Shiomi, D.; Takui, T.; Kubota, M.; Kobayashi, T.; Yakusi, K.; Ouyang, J.; Nakasuji, K. *J. Am. Chem. Soc.* **1999**, *121*, 1619.

10.1021/ja902790q CCC: $40.75

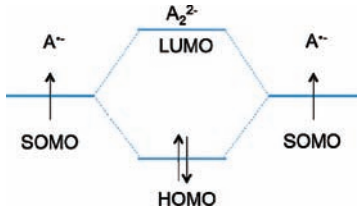

Figure 1. MO diagram arising from the overlap of the SOMO on each $A^{\bullet-}$ to form $[A]_2^{2-}$ (The same diagram can be used for $A^{\bullet+}$ or $A^{\bullet}$.)

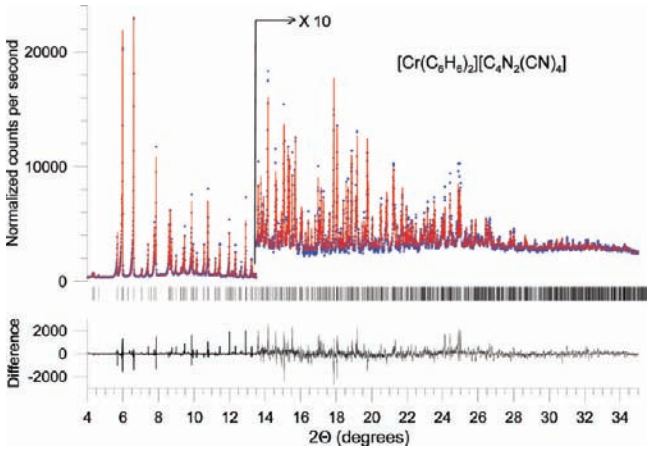

Figure 2. High-resolution synchrotron powder diffraction data (blue) and Rietveld fit of the data (red) for $[Cr(C_6H_6)_2]_2[TCNP]_2$. The lower trace is the difference, measured − calculated, plotted to the same vertical scale (black).

tradimer C−C bonds. Long, 2.9 Å, multicenter C−C bonds have been established for eclipsed cofacial dimers of $[TCNE]^{\bullet-}$, and diamagnetic $[TCNE]_2^{2-}$ is best described as having a 2-electron 4-center ($2e^-/4c$) C−C bond that arises from the overlap of the b_{2g} singly occupied MO (SOMO) on each moiety to form b_{2u} and b_{1g} bonding and antibonding $[TCNE]_2^{2-}$ orbitals.[10a] In addition, dispersion contributes to the bonding.[11] Likewise, long, multicenter bonding has been reported for $[cyanil]_2^{2-}$ (cyanil = tetracyano-1,4-benzoquinone),[10b] as well as cationic $[TTF]_2^{2+}$ (TTF = tetrathiafulvalene),[10c] and neutral [2,5,8-tri-*t*-butylphenalenyl$^{\bullet}$]$_2$[10d] among other examples including $[TCNQ]_2^{2-}$.[12] The generic MO diagram for these multicenter bonded dimers is illustrated for A_2^{2-} in Figure 1.

TCNE {$E°$ [vs SCE(MeCN)] = 0.14 V} and TCNQ [$E°$ = 0.17 V] are easily reversibly reduced, but TCNB and TCNP are more difficult to reduce, as they undergo reversible one electron reductions at the substantially more negative potentials of −0.64 and −0.31 V, respectively.[13] As a consequence, examples of reduced forms of TCNB and TCNP were sought to study the intradimer bonding. While reduced TCNB and TCNP are present in V-based magnets[8a,9] and Ru-based coordination compounds,[13] except for the unusual $[TCNB]_3^{2-}$ trimeric dianion,[8b] they have not been structurally characterized.

$[TCNE]_2^{2-}$ [10a] and $[TTF]_2^{2+}$ [10c] form eclipsed dimers; however, benzene-based $[cyanil]_2^{2-}$ [10b] and $[TCNQ]_2^{2-}$ [12b] dimers have a slipped arrangement. The latter examples can be understood as arising from a compromise between the most attractive SOMO−SOMO intradimer bonding allowed by the symmetry and the electrostatic repulsion of an eclipsed conformation, which provides for good overlap for the slipped arrangement for these species without the steric and electrostatic interactions present for an eclipsed dimer. The a_u symmetry of the SOMO of $[TCNP]^{\bullet-}$, however, does not support a slipped arrangement for $[TCNP]_2^{2-}$; hence, unlike $[cyanil]_2^{2-}$, it should be eclipsed. Herein, we report the synthesis, as well as structural, magnetic, and electronic characterization of $[TCNP]_2^{2-}$.

Experimental Section

$Cr(C_6H_6)_2$ was used as purchased, and TCNP was prepared by a literature route.[14] THF was distilled under nitrogen over sodium and benzophenone. All syntheses were performed in an oxygen-free (<1.0 ppm O_2) drybox. Infrared spectra (±1 cm^{-1}) were recorded on a Bruker Tensor FTIR 37 spectrometer. Elemental analyses were performed by Chemisar Laboratories.

$[Cr(C_6H_6)_2][TCNP]$ was prepared in a drybox (<1 ppm O_2) from TCNP (0.28 mmol) dissolved in 3 mL of THF being added to $Cr(C_6H_6)_2$ (0.28 mmol) dissolved in 2 mL of THF. The color changed from green to dark blue. After stirring overnight, the dark purple precipitate was filtered and washed with THF, and dried under vacuum (yield: 92 mg; 85%). FT-IR (KBr): ν_{CN}; 2174 (s) cm^{-1}. Calcd (obs) for $[Cr(C_6H_6)_2][TCNP]\cdot 0.2THF$, $C_{20.8}H_{13.6}CrN_6O_{0.2}$: %C = 62.03 (61.44), %H = 3.40 (3.24), %N = 20.87 (20.42).

Magnetic susceptibilities were measured in an 1 kOe applied field between 5 and 300 K on a Quantum Design MPMS superconducting quantum interference device (SQUID) equipped with a reciprocating sample measurement system, low field option, and continuous low temperature control with enhanced thermometry features, as previously described.[15]Powder samples for magnetic measurements were loaded in gelatin capsules. In addition to correcting for the diamagnetic contribution from the sample holder, 2 ppm iron impurity, the core diamagnetic correction of -170×10^{-6} emu/mol was used.

Powder diffraction measurements for Rietveld structure analysis were performed at Beamline X16C at the National Synchrotron Light

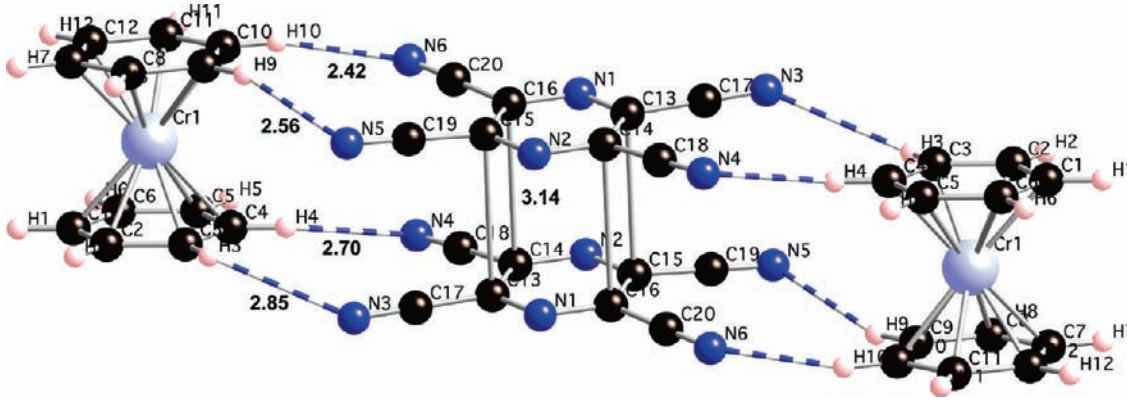

Figure 3. Atom labeling diagram of the $[Cr(C_6H_6)_2]^{\bullet+}$ cation, and cofacial $[TCNP]_2^{2-}$ indicating the shortest $[TCNP]^{\bullet-}\cdots[TCNP]^{\bullet-}$ the shortest H···N distances (Å) in bold numbers. This unit is centrosymmetric, and the nitriles bend slightly out of the plane.

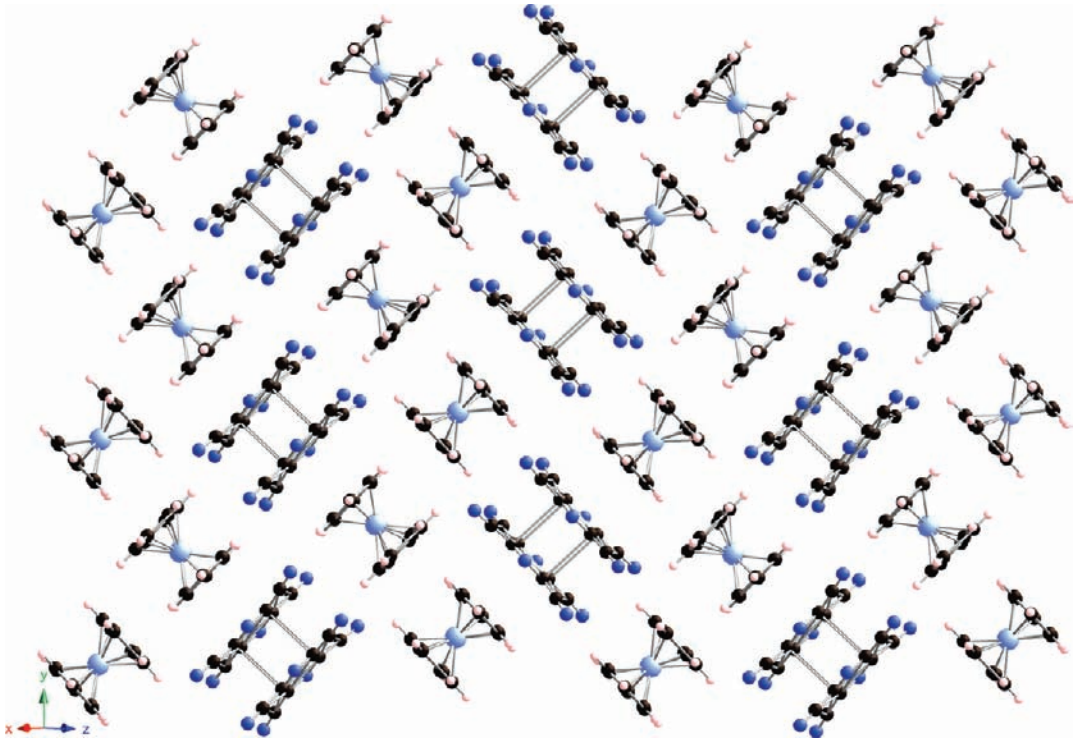

Figure 4. Layered structure $[Cr(C_6H_6)_2][TCNP]$ showing the herringbone motif.

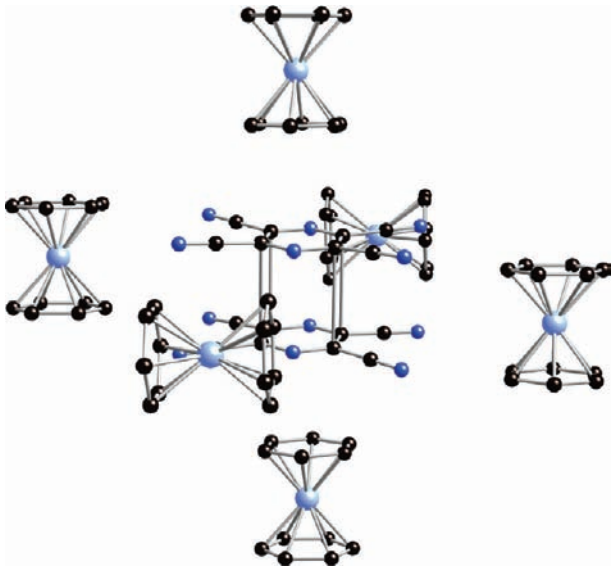

Figure 5. Nearest neighbor interactions for the $[TCNP]_2^{2-}$ with six $[Cr(C_6H_6)_2]^{\bullet+}$ cations (hydrogens not shown for clarity).

Source at Brookhaven National Laboratory. The powdered samples were held in a 1.0 mm diameter thin-wall glass capillary. An X-ray beam of wavelength 0.69862(2) was selected by a Si(111) channel cut, and diffracted X-rays were selected by a Ge(111) analyzer and detected by a scintillation counter. The incident intensity was monitored by an ion chamber and used to normalize the measured signal. The pattern was indexed with TOPAS, solved using DASH, and refine with TOPAS.[16−18]

Theoretical calculations on $[TCNP]^{\bullet-}$, $[TCNP]_2^{2-}$, and $[Cr(C_6H_6)_2]_2[TCNP]_2$ aggregates were evaluated using the B3LYP density functional theory (DFT).[19] As previously shown,[10,11b] this DFT functional is expected to describe the electronic properties of $[TCNP]_2^{2-}$, and the origin of the energetic stability of $[Cr(C_6H_6)_2]_2[TCNP]_2$ aggregates. In all computations the structures

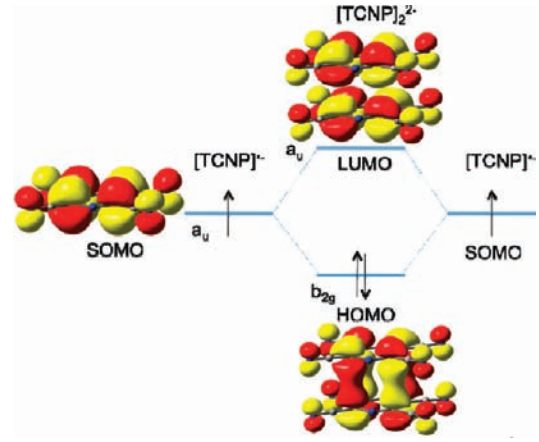

Figure 6. MO diagram arising from the overlap of the a_u SOMOs on each $[TCNP]^{\bullet-}$ forming $[TCNP]_2^{2-}$ b_{2g} bonding and a_u antibonding orbitals.

were based on the crystal structure described herein. The geometry of $[TCNP]_2^{2-}$ was optimized and is stable. As $[TCNP]_2^{2-}$ is diamagnetic (vide infra), only the closed-singlet state is focused upon. All B3LYP calculations were done using the 6-31+G(d) basis set[20]and the Gaussian-03 suite of programs.[21] In all cases the interaction energies were corrected by the basis set superposition error (BSSE) using the counterpoise method.[22,23]

Results and Discussion

The reaction of $Cr(C_6H_6)_2$ and TCNP in THF forms $[Cr(C_6H_6)_2][TCNP]$ as an air sensitive polycrystalline powder.[24]

(11) (a) Jung, Y.; Head-Gordon, M. *Phys. Chem. Chem. Phys.* **2004**, *6*, 2008. (b) Garcia-Yoldi, I.; Mota, F.; Novoa, J. J. *J. Comput. Chem.* **2007**, *28*, 326.

(12) (a) Huang, J.; Kingsbury, S.; Kertesz, M. *Phys. Chem. Chem. Phys.* **2008**, *10*, 2625. (b) Herbstein, F. H.; Kapon, M. *Crystallogr. Rev.* **2008**, *14*, 3. (c) Garcia -Yoldi, I.; Miller, J. S.; Novoa, J. J. *J. Phys. Chem.* (accepted).

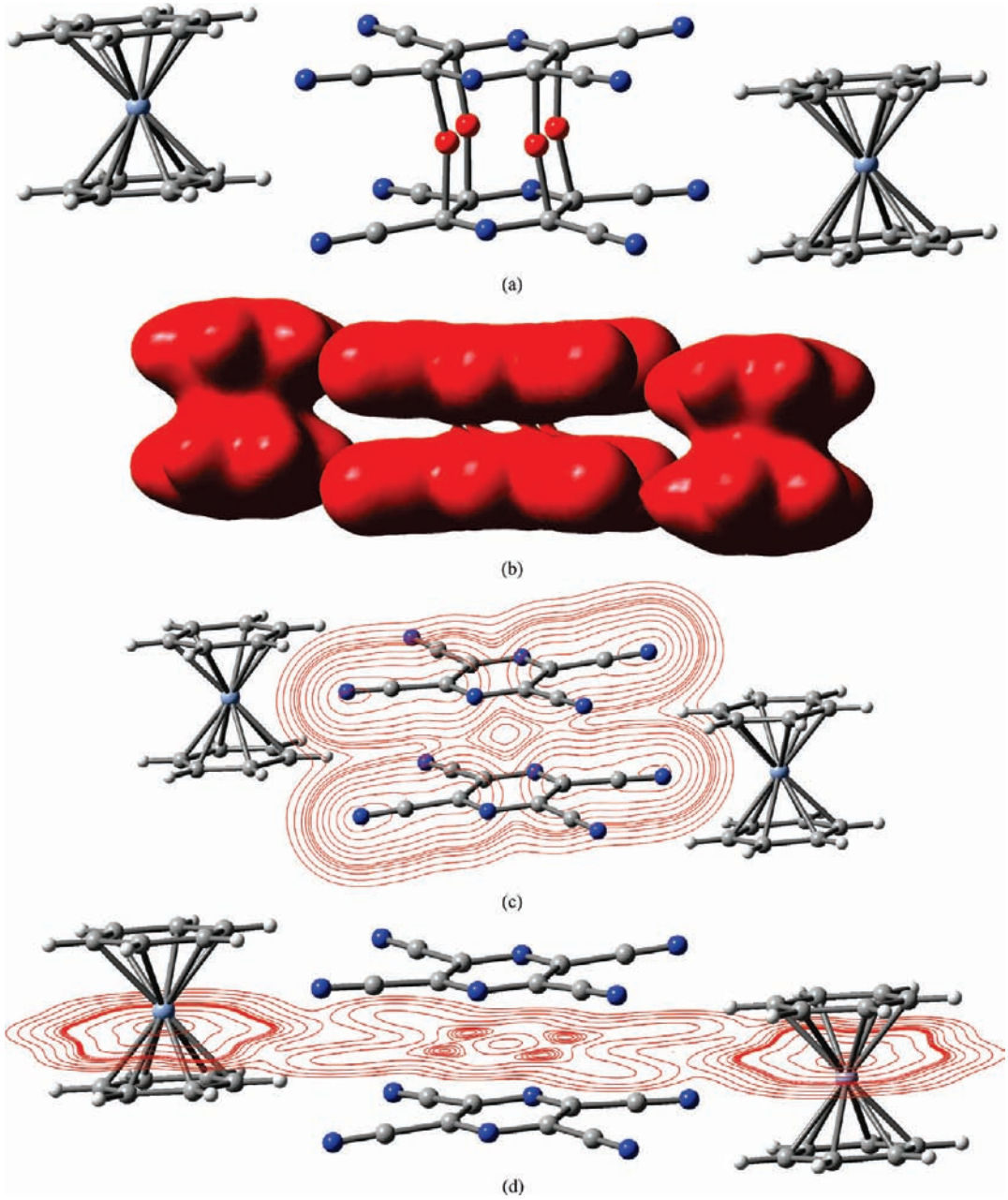

Figure 7. Isosurface of 0.075 atomic units for the B3LYP electron density of the $[Cr(C_6H_6)_2]_2[TCNP]_2$ aggregate, which graphically indicates the position of the four (3,−1) bond critical points (red spheres) (a) by the four funnels that connect each the two $[TCNP]^-$ moieties (b); cut of the computed electron density along the plane that passes through four nitrile groups to show the absence of funnels (bond critical points) involving the nitrile groups (c); and cut of the electron density along the plane that passes through the equator of the $[TCNP]_2^{2-}$ dimer (d). These plots are very similar to those obtained when analyzing the density of a $[TCNP]_2^{2-}$ dimer (Figure S1 in the Supporting Information).

The strong ν_{CN} absorption occurs at 2174 cm^{-1} indicative of reduced TCNP {it occurs at 2223, 2188, and 2136 cm^{-1} for $V^{II}[TCNP]_2$ and 2254 (sh) and 2248 (m) cm^{-1} for TCNP°}, which among other possibilities could be the isolated $[TCNP]^{\bullet-}$ or its σ or π dimer, as has been established for reduced TCNE.[5]

Structure. Attempts to grow single crystals were unsuccessful, but high-resolution X-ray powder diffraction patterns (Figure 2) were collected, and Rietveld refinements of the data, Table 1, enabled the determination of the structure. In the refinement, $Cr(C_6H_6)_2$ was constrained to have C_6 symmetry; TCNP, C_{2v}. The atom-labeling diagram is shown in Figure 3.

The structure consists of the $[Cr(C_6H_6)_2]^{\bullet+}$ cation and a centrosymmetric π dimer of $[TCNP]_2^{2-}$ (Figure 3). The TCNP fragment has $C(sp^2)-N$, $C(sp^2)-C(sp^2)$, $C(sp^2)-C(sp)$, and $C(sp)-N$ distances of 1.33, 1.45, 1.43, and 1.14 Å, respectively. The C(sp) is linear, and the NCC(sp), CCC, and NCC angles

(13) Moscherosch, M.; Waldhor, E.; Binder, H.; Kaim, W.; Fiedler, J. *Inorg. Chem.* **1995**, *34*, 4326.
(14) Begland, R. W.; Hartter, D. R.; Donald, D. S.; Cairncross, A.; Sheppard, W. A. *J. Org. Chem.* **1974**, *39*, 1235.
(15) Brandon, E. J.; Rittenberg, D. K.; Arif, A. M.; Miller, J. S. *Inorg. Chem.* **1998**, *37*, 3376.
(16) Bruker AXS. *TOPAS V3: General profile and structure analysis software for powder diffraction data—User's Manual*; Bruker AXS: Karlsruhe, Germany, 2005.
(17) Coelho, A. A. *J. Appl. Crystallogr.* **2000**, *33*, 899.
(18) David, W. I. F.; Shankland, K.; van de Streek, J.; Pidcock, E.; Motherwell, W. D. S.; Cole, J. C. *J. Appl. Crystallogr.* **2006**, *39*, 910.

Table 1. Summary of Crystallographic Parameters for $[Cr(C_6H_6)_2][TCNP]$

formula	$C_{20}H_{12}CrN_6$	Z	4
MW, g/mol	388.36	space group	$P2_1/c$ (No. 14)
a, Å	9.3374(2)	ρ_{calc}, g/cm^3	1.480
b, Å	10.8037(2)	R_{wp} [a,b]	0.0675
c, Å	17.3964(4)	R_{exp} [b,c]	0.0287
β, deg	95.327(1)	T, K	296
V, Å^3	1747.34(6)	GOF (R_{wp}/R_{exp})	2.355
λ, Å	0.69862(2)		

[a] $R_{wp} = \{[\sum_i w_i(y_i^{calc} - y_i^{obs})^2]/[\sum_i w_i(y_i^{obs})^2]\}^{1/2}$. [b] y_i^{calc} and y_i^{obs} are the calculated and observed intensities at the ith point in the profile, normalized to monitor intensity. The weight w_i is $1/\sigma^2$ from the counting statistics, with the same normalization factor. N is the number of points in the measured profile − number of parameters. [c] $R_{exp} = [N/(\sum_i w_i(y_i^{obs})^2]^{1/2}$.

around the C(sp^2) atom are 118, 119, and 123°, respectively, while the CNC angle averages 115°; thus, the reduced TCNP unit is slightly nonplanar as the nitriles bend away from the ring by 5.0(10)° (e.g., 180° − ∠C14−C16−C20). This bending is comparable to that reported for $[TCNE]_2^{2-}$,[10a] and larger than observed for $[cyanil]_2^{2-}$,[10b] while it does not occur for $[TCNQ]_2^{2-}$.[12] The pyrazine unit was allowed to bend along the N1−N2 seam, but the refinement found it to be planar. Furthermore, $[TCNP]_2^{2-}$ has cofacial intrafragment sub van der Waals C···C and N···N separations of 3.14(3) Å with intradimer C(nitrile)−C(nitrile) and N(nitrile)−N(nitrile) separations of 3.29(3) and 3.42(3) Å, respectively, that increase with the distance from the center of the molecule, due to nitriles bending away from center of the molecule. The structure of $[Cr(C_6H_6)_2]^{\bullet+}$ is typical,[25a] with a Cr−C distance of 2.15(2) Å, ring centroid−Cr distance of 1.62(2) Å, but the benzene rings are staggered by an unusually large 21(1)°.

The solid-state motif is composed of layers possessing a herringbone arrangement of $[Cr(C_6H_6)_2][TCNP]_2[Cr(C_6H_6)_2]$ units, Figure 4. These units have the C_6-rings both nominally parallel and perpendicular to the nominal TCNP-plane. The former has Cr···N separations ranging from 4.84 to 5.31 Å (Figure 3), while the latter has Cr···N separations exceeding 6 Å. Nearest neighbor cations are nominally rotated 90° with respect to each other and have Cr···Cr separations of 6.67 Å. Each $[TCNP]_2^{2-}$ dimer is surrounded by six nearest neighbor $[Cr(C_6H_6)_2]^{\bullet+}$ cations, Figure 5. Noninteracting $[TCNP]_2^{2-}$ dimers occur along the a-axis, Figure 4, with the shortest interdimer N(sp)···N(sp) separation being 4.05 Å, but there is no overlapping between the dimer orbitals.

Magnetic Properties. Magnetic studies show that $[TCNP]_2^{2-}$ is diamagnetic, which is similar to that previously reported for $[TCNE]_2^{2-}$.[10a] The EPR spectrum of the solid has a single absorption at $g = 1.991(1)$ that is characteristic Cr^I,[25a] and lacks an absorption assignable to $[TCNP]^{\bullet-}$. The room temperature value of χT is 0.374 emu K/mol,[25b] in accord with $S = 1/2$ paramagnetic cation and its observed g value. The lack of antiferromagnetic coupling among the $S = 1/2$ cations is attributed to the large separations of the SOMO d_{z^2} orbitals.

Electronic Structure and Stability of $[TCNP]_2^{2-}$. The RB3LYP-computed interaction energy for $[TCNP]_2^{2-}$ for the closed-shell singlet state crystal geometry is repulsive by 57.5 kcal/mol (58.9 kcal/mol, when the BSSE is corrected); i.e. it is unstable with respect to the dissociation of into its fragments. As shown for $[TCNE]_2^{2-}$,[11] B3LYP calculations do not properly account for the dispersion component of the interaction energy, but its inclusion at the MCRQDPT2/CASSCF(2,2) level results in a more metastable minimum. A similar stabilizing effect of reducing the repulsive nature of these ion radicals is expected to occur for $[TCNP]_2^{2-}$. Therefore, as previously reported for ion radical dimers,[10,12b] the bonding component that originates from the SOMO−SOMO overlap of the radical ions is insufficient to compensate for the electrostatic repulsion associated to the ionic nature of these radicals. Hence, its existence in the solid state should be attributed to the presence of energetically stable aggregates that contain these dimers, whose stability primarily originates in the $cation^+\cdots anion^-$ attractive interactions whose sum exceeds the sum of the $cation^+\cdots cation^+$ and $anion^-\cdots anion^-$ repulsive interactions.[11]

To validate the previous ideas, the energetic stability of $[TCNP]_2^{2-}$ dimers found in the $[Cr(C_6H_6)_2]_2[TCNP]_2$ aggregate (Figure 3) was computed. The results of B3LYP/6-31+G(d) calculations indicated that the aggregate is stable against its dissociation in its four constituent fragments by 99.7 kcal/mol (97.4 when the BSSE is corrected). This stability was evaluated from the results of computing the $anion^-\cdots anion^-$, $cation^+\cdots cation^+$, and the four nearest neighbor $cation^+\cdots anion^-$ pairwise interactions. At the B3LYP/6-31+G(d) level, the values for these interactions are respectively 57.5, 81.4, −53.1, −52.9, −53.1, and −52.9 kcal/mol, totaling −73.1 kcal/mol (the corresponding BSSE-corrected values are 58.9, 81.4, −52.3, −52.4, −52.5, and −52.4 kcal/mol, totaling −96.3 kcal/mol). This is qualitatively in accord with the −99.7 kcal/mol interaction energy computed above, and the differences indicate the importance of the polarization and non-nearest neighbor pairwise (and higher order) interactions. Therefore, the stability of the $[Cr(C_6H_6)_2]_2[TCNP]_2$ aggregates can be mostly attributed to the $[TCNP]^{\bullet-}\cdots cation^+$ interactions, whose sum exceeds the sum of the $[TCNP]^{\bullet-}\cdots[TCNP]^{\bullet-}$ and $cation^+\cdots cation^+$ repulsions and this is expected to increase when the stabilizing dispersion is properly accounted for in the $anion^-\cdots anion^-$ interaction.

As a consequence of the short 3.14 Å sub van der Waals intradimer separation, the computed electronic structure of $[TCNP]_2^{2-}$ shows that the SOMO of each $[TCNP]^{\bullet-}$ fragment overlap to form bonding and antibonding orbitals, Figure 6. Note that due to the nodes at the ring nitrogens, contribution to the bonding overlap does not occur for these atoms. Therefore, as a consequence of the SOMO−SOMO overlap, $[TCNP]_2^{2-}$ has the typical MO diagram found on other ion radicals dimers, Figure 1. This diagram explains the closed-shell singlet ground state and the diamagnetic properties of $[TCNP]_2^{2-}$ dimers. Therefore, a long, multicenter bond is present for $[TCNP]_2^{2-}$. Its properties can be evaluated from an atoms-in-molecule analysis[26] of the B3LYP-computed electron

(19) B3LYP is a density functional obtained by taking the three parameter non-local exchange functional of Becke and the non-local correlation functional of Lee−Yang−Parr:(a) Becke, A. D., *J. Chem. Phys.* **1993**, *98*, 5648. (b) Lee, C.; Yang, W.; Parr, R. G. *Phys. Rev. B* **1988**, *37*, 785.

(20) A basis set built by adding diffuse functions to the 6-31G(d) basis set: Ditchfield, R.; Hehre, W. J.; Pople, J. A. *J. Chem. Phys.* **1971**, *54*, 724.

(21) Frisch, M. J.; et al.; *Gaussian-03, Revision-C.02*; Gaussian, Inc.: Wallingford, CT, 2004. See Supporting Information for the full reference.

(22) Boys, S. F.; Bernardi, F. *Mol. Phys.* **1970**, *19*, 553.

(23) BSSE (basis-set-superposition error) is the error introduced by the use of finite basis sets when computing the interaction energy between two molecules. As originally shown by Boys and Bernardi,[22] it can be corrected by using the counterpoise correction. While the validity has been questioned, it has shown to be valid on the basis of analytical[23a] and numerical[23b] studies when basis sets of good quality are used. (a) van Duijneveldt, F. B.; van Duijneveldt-van de Rijdt, J. G. C. M.; van Lenthe, J. H. *Chem. Rev.* **1994**, *94*, 1873. (b) Novoa, J. J.; Planas, M.; Whangbo, M.-H. *Chem. Phys. Lett.* **1994**, *225*, 240.

Table 2. Summary of Long, Multicenter Bonding Observed for $[TCNE]_2^{2}$, $[TCNQ]_2^{2}$, $[Cyanil]_2^{2}$, and $[TCNP]_2^{2-}$ Ordered in Terms of Their Shortest Intradimer Separation

dimer	intradimer separation, Å	rel orientation	eclipsed atoms	overlap bonding type $2e^-/nc$, n	ref
$[cyanil]_2^{2-}$	2.88	slipped	14	10 (8C +2O)	10b
$[TCNE]_2^{2-}$	2.89	eclipsed	20	4C	10a
$[TCNP]_2^{2-}$	3.14	eclipsed	28	8C	this work
$[TCNQ]_2^{2-}$	3.3	slipped	18[a,12a]−32[12b]	20 (12C+8N)	12b

[a] E.g.: Goldberg, S. Z.; Spivack, B.; Stanley, G.; Eisenberg, R.; Braitsch, D. M.; Miller, J. S.; Abkowitz, M. *J. Am. Chem. Soc.* **1977**, *99*, 110.

density of $[TCNP]_2^{2-}$ and $[Cr(C_6H_6)_2]_2[TCNP]_2$ aggregates. This analysis shows in both cases four (3,−1) bond critical points that connect the four carbon atoms from each ring with each other (Figure 7a,b) in accord with the bonds drawn in Figure 3. These bond critical points have a density of 1.26×10^{-2} atomic units, and a positive Laplacian (1.26×10^{-2} atomic units) similar to those found in other long bonds.[10a,b,12b] The similarity in the atom-in-molecule analysis when the $[TCNP]_2^{2-}$ dimer is isolated or in $[Cr(C_6H_6)_2]_2[TCNP]_2$ aggregates indicates that the polarization induced by the cations in the $[TCNP]_2^{2-}$ density does not alter the main features of the density topology in these dimers. This is graphically demonstrated by looking at the 2-D cuts of the density plotted in Figures 7c,d and S1 in the Supporting Information. Note, however, that there eight new H···N bond critical points, two for each cation$^+$···$[TCNP]^{\bullet-}$ interaction. Given the computed energetic stability of the cation$^+$···$[TCNP]^{\bullet-}$ interaction, eight C−H$^+$···N$^-$ bonding interactions can be said to exist. The previous results indicate that the long, multicenter intradimer bond in $[TCNP]_2^{2-}$ involves only four C···C components (bond critical points) and is a $2e^-/8c$ bond (Figure 7a,b). The absence of any N···N components could be attributed to an decrease of the electron density due to the shape of the SOMO in that region, or to contraction of the atomic electron density on N compared to C, as corresponds to its higher electronegativity. Based on a comparison with other molecules (vide infra) the former is more important.

Conclusion

$[TCNP]_2^{2-}$ has been experimentally observed and computationally studied. B3LYP/6-31+G(d) calculations on isolated $[TCNP]_2^{2-}$ dimers and in representative $[Cr(C_6H_6)_2]_2[TCNP]_2$ aggregates indicate that interaction energies for an isolated $[TCNP]_2^{2-}$ dimer at the crystal geometry are repulsive, and their stability primarily originates in the cation$^+$···anion$^-$ attractive interactions whose sum exceeds the sum of the cation$^+$···cation$^+$ and anion$^-$···anion$^-$ repulsive interactions. As a consequence, the two radical anions can approach each other such that their SOMOs can overlap to form bonding and antibonding orbitals (Figures 1 and 6) in a similar manner to that produced in the usual covalent bonds. This stabilization and overlap also occurs for $[TCNE]_2^{2-}$, $[TCNQ]_2^{2-}$, and $[cyanil]_2^{2-}$ (Table 2). In all cases the bonding orbital has two electrons and the dimers have closed-shell diamagnetic ground states, as observed. The computational results for $[TCNP]_2^{2-}$ are compared with previous results obtained on similar anion radical dimers that exhibit long, multicenter bonding, namely, $[TCNE]_2^{2-}$, $[TCNQ]_2^{2-}$, and $[cyanil]_2^{2-}$ (Table 2). $[TCNP]_2^{2-}$ has an intradimer separation that exceeds that of both $[TCNE]_2^{2-}$and $[cyanil]_2^{2-}$, but is less than that observed for $[TCNQ]_2^{2-}$. $[TCNP]_2^{2-}$ like $[TCNE]_2^{2-}$ has eclipsed conformations, while $[TCNE]_2^{2-}$and $[cyanil]_2^{2-}$ have slipped orientations. As the intradimer distance increases, the overlap between two anion radical SOMOs decreases (for the same orientation), but the atom−atom Coulombic repulsion should also decrease. Hence, the optimum geometry of these dimers and intradimer separation depends in a complex manner on the SOMO−SOMO overlap and the Coulombic repulsion. Each of these dianionic dimers has long, multicenter two electron bonds, but the number of centers differ. This reflects the differences in the number of atoms, topology, overlap and electron densities of each radical anion that dimerizes. Also relevant is the coplanarity of the nitrile groups with respect to the plane of the radical anions. They are coplanar for $[TCNQ]_2^{2-}$, and hence contribute to the multicenter bonding.[12c] In contrast, they bend away for $[TCNE]_2^{2-}$, $[cyanil]_2^{2-}$, and $[TCNP]_2^{2-}$ and do not contribute to the multicenter bonding. Note, however, in all cases there is no C(sp)···C(sp) contribution to the long bond. Finally, the number of eclipsed atoms is not equal to the number of bond components found in the atoms-in-molecules analysis (Table 2), reinforcing the importance of the topology of the fragments SOMO on the total density of these dimers.

Acknowledgment. The authors gratefully acknowledge preliminary studies by J. D. Bagnato (Utah), as well as assistance from Y. J. Jiang (Utah), A. C. McConnell (Utah), F. Mota (Barcelona), and E. Shurdha (Utah), as well as the computational allocation generously provided by the NIH (No. NCRR 1 S10 RR17214-01) on the Arches Metacluster administered by the University of Utah Center for High Performance Computing, and the support from the NSF (No. 0553573) and DOE (No. DE FG 03-93ER45504); use of the National Synchrotron Light Source, Brookhaven National Laboratory, was supported by the U.S. DOE, BES (DE-AC02-98CH10886). J.J.N. was supported by the Spanish Science and Education Ministry (MAT2008-02032/MAT, BQU2002-04587-C02-02 and UNBA05-33-001, and Ph.D. grant to IG-Y) and the CIRIT (2001SGR-0044 and 2005-PEIR-0051/69). Computer time was also provided by CESCA and BSC.

Supporting Information Available: Powder X-ray crystallographic data for $[Cr(C_6H_6)_2]_2[TCNP]_2$ (CCDC #718516) in CIF format. Selected bond distances and angles, details of the B3LYP-computed electron density of an isolated $[TCNP]_2^{2-}$ dimer and its the bond critical points. The geometries (in Cartesian coordinates) of the calculated structures. Complete ref 21. This material is available free of charge via the Internet at http://pubs.acs.org.

JA902790Q

(24) Reduction of TCNP with $CoCp_2^*$, KC_8, and $[(Me_2N)_2C]_2$ formed materials with different ν_{CN} absorptions indicating that a form of reduced TCNP other than $[TCNP]_2^{2-}$ was present.

(25) (a) Miller, J. S.; O'Hare, D. M.; Chakraborty, A.; Epstein, A. J. *J. Am. Chem. Soc.* **1989**, *111*, 7853. (b) Corrected for 2 ppm Fe impurity.

(26) (a) Bader, R. F. *Atoms in Molecules. A Quantum Theory*; Clarendon Press: Oxford, 1990. (b) All atoms-in-molecules calculations were performed using PROAIM: Biegler-Konig, F. W.; Bader, R. F. W.; Tang, T. H. *J. Comput. Chem.* **1982**, *3*, 317.